ORIGINAL RESEARCH ARTICLE

Overexpression of endothelial β₃-adrenergic receptor induces diastolic dysfunction in rats

Justine Dhot[1†], Marine Ferron[1†], Valentine Prat[1†], Antoine Persello[1], David Roul[1], David Stévant[1], Damien Guijarro[1], Nicolas Piriou[1], Virginie Aillerie[1], Angélique Erraud[1], Gilles Toumaniantz[1], Morteza Erfanian[1], Angela Tesse[1], Amandine Grabherr[1], Laurent Tesson[2,3], Séverine Menoret[2,3,4], Ignacio Anegon[2,3], Jean-Noël Trochu[1], Marja Steenman[1], Michel De Waard[1,5], Bertrand Rozec[1], Benjamin Lauzier[1*,‡] and Chantal Gauthier[1‡]

[1]*Université de Nantes, CHU Nantes, CNRS, INSERM, l'institut du thorax, Nantes, F-44000, France;* [2]*Centre de Recherche en Transplantation et Immunologie UMR1064, INSERM, Université de Nantes, Nantes, France;* [3]*Institut de Transplantation Urologie Néphrologie (ITUN), CHU Nantes, Nantes, France;* [4]*CNRS, SFR de Nantes, Nantes, France;* [5]*LabEx 'Ion Channels, Science & Therapeutics', Nice, France*

Abstract

Aims   Diastolic dysfunction is common in cardiovascular diseases, particularly in the case of heart failure with preserved ejection fraction. The challenge is to develop adequate animal models to envision human therapies in the future. It has been hypothesized that this diastolic dysfunction is linked to alterations in the nitric oxide (•NO) pathway. To investigate this issue further, we investigated the cardiac functions of a transgenic rat model (Tgβ₃) that overexpresses the human β₃-adrenoceptor (hβ₃-AR) in the endothelium with the underlying rationale that the •NO pathway should be stimulated in the endothelium.

Methods and results   Transgenic rats (Tgβ₃) that express hβ₃-AR under the control of intercellular adhesion molecule 2 promoter were developed for a specific expression in endothelial cells. Transcriptomic analyses were performed on left ventricular tissue from 45-week-old rats. Among all altered genes, we focus on •NO synthase expression and endothelial function with arterial reactivity and evaluation of •NO and $O_2^{\bullet-}$ production. Cardiac function was characterized by echocardiography, invasive haemodynamic studies, and working heart studies. Transcriptome analyses illustrate that several key genes are regulated by the hβ₃-AR overexpression. Overexpression of hβ₃-AR leads to a reduction of Nos3 mRNA expression (-72%; $P < 0.05$) associated with a decrease in protein expression (-19%; $P < 0.05$). Concentration-dependent vasodilation to isoproterenol was significantly reduced in Tgβ₃ aorta (-10%; $P < 0.05$), while •NO and $O_2^{\bullet-}$ production was increased. In the same time, Tgβ₃ rats display progressively increasing diastolic dysfunction with age, as shown by an increase in the E/A filing ratio [1.15 ± 0.01 (wild type, WT) vs. 1.33 ± 0.04 (Tgβ₃); $P < 0.05$] and in left ventricular end-diastolic pressure [5.57 ± 1.23 mmHg (WT) vs. 11.68 ± 1.11 mmHg (Tgβ₃); $P < 0.05$]. In isolated working hearts, diastolic stress using increasing preload levels led to a 20% decrease in aortic flow [55.4 ± 1.9 mL/min (WT) vs. 45.8 ± 2.5 mL/min (Tgβ₃); $P < 0.05$].

Conclusions   The Tgβ₃ rat model displays the expected increase in •NO production upon ageing and develops diastolic dysfunction. These findings provide a further link between endothelial and cardiac dysfunction. This rat model should be valuable for future preclinical evaluation of candidate drugs aimed at correcting diastolic dysfunction.

Introduction

The high prevalence, mortality, and health costs associated with heart failure (HF) make it a major public health issue. Several terminologies exist to classify patients with HF according to their ejection fraction (EF).[1,2] At present, patients with HF with preserved EF (HFpEF) are more difficult to manage clinically due to the complexity of the phenotypes underlying this pathology. Indeed, several co-morbidities are described in HFpEF patients, such as high blood pressure, obesity, diabetes, atrial fibrillation, ageing, and the influence of gender on the disease, all of which complicate diagnosis and the identification of effective therapeutic targets.[3] The common feature of all HFpEF phenotypes is diastolic dysfunction with altered relaxation and increased filling pressures.[4] The early phase of diastolic dysfunction is generally asymptomatic. When patients become symptomatic, they show a decrease in their tolerance to exercise or to stress conditions leading to cardiac decompensation.[5] Because HFpEF remains a poorly understood pathology with no treatment to improve patient survival, it is important to develop animal models that best recapitulate the human phenotypes. Such HFpEF models may in turn help understand how diastolic dysfunction is generated over time within this pathology and provides hope for accelerated drug discovery. Basic and clinical studies have highlighted that the endothelium plays a role in the pathophysiology of HFpEF and the observed diastolic dysfunction.[6,7] Endothelial cells may be a key factor in the development of the diastolic dysfunction with a significant involvement of nitric oxide ($^\bullet$NO) and $^\bullet$NO synthase (NOS).

Indeed, Schiattarella *et al.* showed that an increase in iNOS activity and expression can drive the diastolic dysfunction of HFpEF through an increase in $^\bullet$NO production. [8] Considering the fact that $^\bullet$NO production is mainly due to Gαi–$^\bullet$NO–cGMP activation and that this pathway is coupled to the expression and activity of β$_3$-adrenergic receptors (β$_3$-AR),[9,10] we decided to investigate how overexpression of this receptor in the endothelium may influence $^\bullet$NO production and whether it may lead to a new and original model of HFpEF. For that purpose, we have generated a rat model overexpressing the human β$_3$-AR (hβ$_3$-AR) within endothelial cells (Tgβ$_3$), and we evaluated how it impacted $^\bullet$NO production and myocardial function. We demonstrate that the excessive $^\bullet$NO production is indeed associated with a progressive alteration of diastolic function upon ageing.

Materials and methods

All animal experimental protocols were approved by the Pays de la Loire Ethical Committee and were performed in accordance with the French law on animal welfare, EU Directive 2010/63/EU for animal experiments, the National Institutes of Health Guide for the Care and Use of Laboratory Animals (National Institutes of Health Pub. No. 85-23, revised 2011), and the 1964 Declaration of Helsinki and its later amendments. In functional protocols, both male and female animals were investigated. All experimental procedures performed are available in detail in the Supporting Information.

Figure 1 β-Adrenergic receptor transcript expression. Transcript levels of hβ$_3$-AR mRNA (A) and rat β$_1$-AR, β$_2$-AR, and β$_3$-AR mRNA (B), in wild-type (WT) (*n* = 8) and Tgβ$_3$ (*n* = 13) rats. Reverse transcription PCR assays were performed on whole heart, and de-endothelialized or intact aorta tissue extracts (C), and isolated cardiomyocytes (D). hadrb3, human β$_3$-AR. Data are expressed as mean ± standard error of the mean, $^*P < 0.05$.
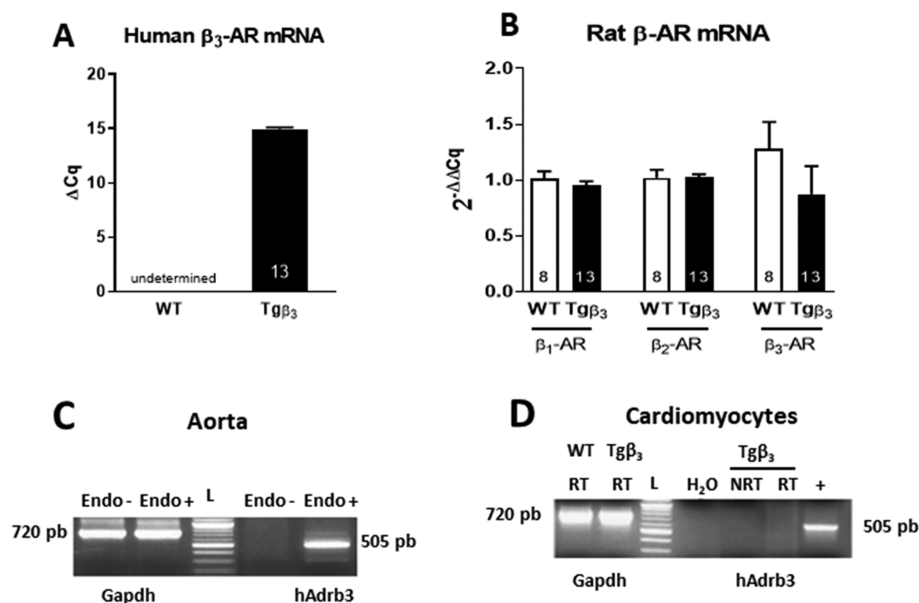
Results

Rat model overexpressing human β₃-adrenoceptor in endothelial cells

To confirm cardiac hβ₃-AR expression in our model, quantitative reverse transcription PCR analyses were conducted on whole-heart extract samples. Our assays showed a high level of hβ₃-AR mRNA in Tgβ₃ whole-heart samples (*Figure 1A*). Expression of the transgene did not impact the expression of endogenous β₁-AR, β₂-AR, and β₃-AR (*Figure 1B*). To confirm endothelial expression of the inserted gene, reverse transcription PCR was performed on aortas and isolated cardiomyocytes. The presence of hβ₃-AR transcripts was confirmed in entire Tgβ₃ aortas (*Figure 1C*), while it was not detected in wild-type (WT) aortic tissue nor in the aortas of Tgβ₃ rats in which the endothelium was removed. Conversely, hβ₃-AR transcripts were absent in isolated cardiomyocytes (*Figure 1D*), confirming that hβ₃-AR mRNA could be expressed in the endothelial cells of Tgβ₃ rats, but further study should be performed to confirm. These results agree with the use of the intercellular adhesion molecule 2 promoter that should restrict expression to the endothelium. Analyses of protein expression levels using a β₃-AR-specific antibody illustrate that protein expression increased over time between 15 and 45 weeks of age (Supporting Information, *Figure S1*). Like many others, this antibody does not distinguish between the rat and human isoforms of β₃-AR, but it is reasonable to assume that the increased level of protein expression is due to the transgene.

Transcriptomic analyses of transgenic rats

In order to investigate the impact of hβ₃-AR overexpression in the endothelium on cardiac gene expression, we turned towards transcriptomic analyses. Using significance analysis of microarrays with false discovery rate = 0.05, we identified 241 transcripts that were differentially expressed in Tgβ₃ rats compared with WT rats (Supporting Information, '45wk males differential'). Among these genes, 15 of them were up-regulated, whereas 226 other ones were down-regulated (*Figure 2A*). The data indicate an up-regulation of several transcripts involved in collagen formation and in the regulation of the metabolism in Tgβ₃ rats. The main down-regulated transcripts were involved in the reactive oxygen pathway and the immune system. Further analyses of the data by gene set enrichment analysis underlined these findings: when using all gene sets as input, 49 gene sets were significantly up-regulated in Tgβ₃ rats and 78 gene sets were significantly down-regulated. Most of the up-regulated gene sets were associated with the extracellular matrix, indicating an activation of fibrotic pathways in the transgenic rats (*Figure 2B* and *2C*) that display the most significant gene sets. To focus on the

•NO pathway, gene set enrichment analysis was also performed on endothelial NOS (eNOS)-associated and inducible NOS (iNOS)-associated gene sets only. When analysing eNOS-associated gene sets, a positive association was found with the CHEN_LVAD_OF_FAILING_FAILING_HEART_UP gene set (*Figure 2D*). Although this gene set does not contain eNOS, eNOS was found to be up-regulated in the corresponding study.[11] Analysis of iNOS-associated gene sets pointed towards the implication of reactive oxygen biosynthesis (*Figure 2E*). We decided to perform a more in-depth analysis of the eNOS pathways in this animal model.

Transgenic rats display a dysfunction in endothelial nitric oxide synthase pathways

Imbalance in nitric oxide synthase pathway

To investigate the potential physiopathological mechanism involved in our model, mRNA analyses of neuronal NOS (nNOS) (Nos1) and iNOS (Nos2) were performed on WT and Tgβ₃ rats on the left ventricle. The analysis shows no significant alteration concerning the mRNA levels for Nos1 and Nos2 (*Figure 3A* and *3B*), but we detected a significant decrease in eNOS (Nos3) mRNA expression in Tgβ₃ rats (*Figure 3C*). Interestingly, the protein levels of nNOS and iNOS were significantly increased in Tgβ₃ rats (*Figure 3D* and *3E*). In contrast, the eNOS levels were decreased (*Figure 3F*), without an alteration of the phosphorylation level of eNOS (*Figure 3G*). We conclude that overexpression of hβ₃-AR should lead to a significant imbalance in NOS pathways.

Impairment of nitric oxide production and endothelial dysfunction

To confirm a possible endothelial dysfunction linked to these changes in NOS expression levels, we investigated the vascular function in response to aortic isoproterenol in Tgβ₃ animals. We found that the response to isoproterenol was reduced in Tgβ₃ animals (*Figure 4A*). This decrease in vasorelaxation is counterintuitively related to an increase in •NO and $O_2^{•-}$ productions in these aortas (*Figure 4B* and *4C*), suggesting that the balance of expression of NOS subtypes in the endothelium plays an important role.

All these contextual findings, at both the transcriptome and protein levels, represented strong incentives to carefully investigate potential cardiac pathologies in this rat model.

Transgenic rats develop a phenotype similar to age-related diastolic dysfunction in heart failure with preserved ejection fraction models

General characteristics

To examine the impact of the overexpression of hβ₃-AR in the endothelium on the rat cardiac phenotype, echocardiography

Figure 2 Transcriptome analysis on the left ventricle. Hierarchical clustering of microarray data based on the 241 transcripts differentially expressed between Tgβ3 and wild-type (WT) rats (A). Gene expression is presented as a coloured matrix, where each row represents a gene and each column represents a sample. Green, black, and red correspond to lower values, median values, and higher values, respectively. (B–E) Gene set enrichment analysis enrichment plots and heat maps based on gene expression profiles from Tgβ3 and WT rats. Only genes from the gene set enrichment analysis core enrichment are displayed in the heat maps.
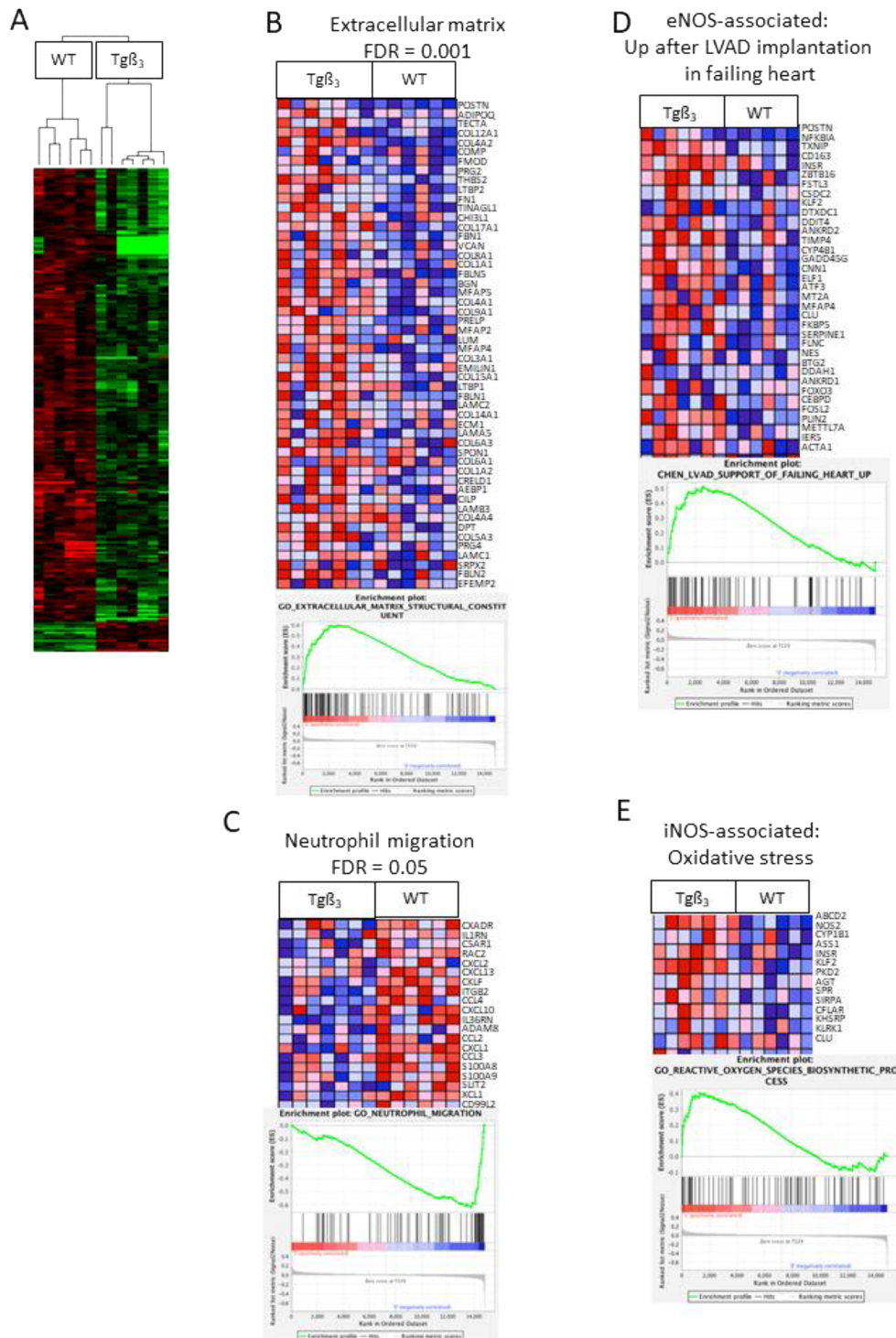
Figure 3 Changes in NOS transcripts and protein expression and phosphorylation on the left ventricle. nNOS (Nos1) (A), iNOS (Nos2) (B), and nNOS (Nos3) (C) mRNA levels in wild-type (WT) (n = 8) and Tgβ_3 (n = 13) rats. Western blot analysis was performed to study total expression of nNOS (D), iNOS (E), and eNOS (F) and level of phosphorylated Ser1177 eNOS (G). Data are expressed as mean ± standard error of the mean. $^*P < 0.05$.
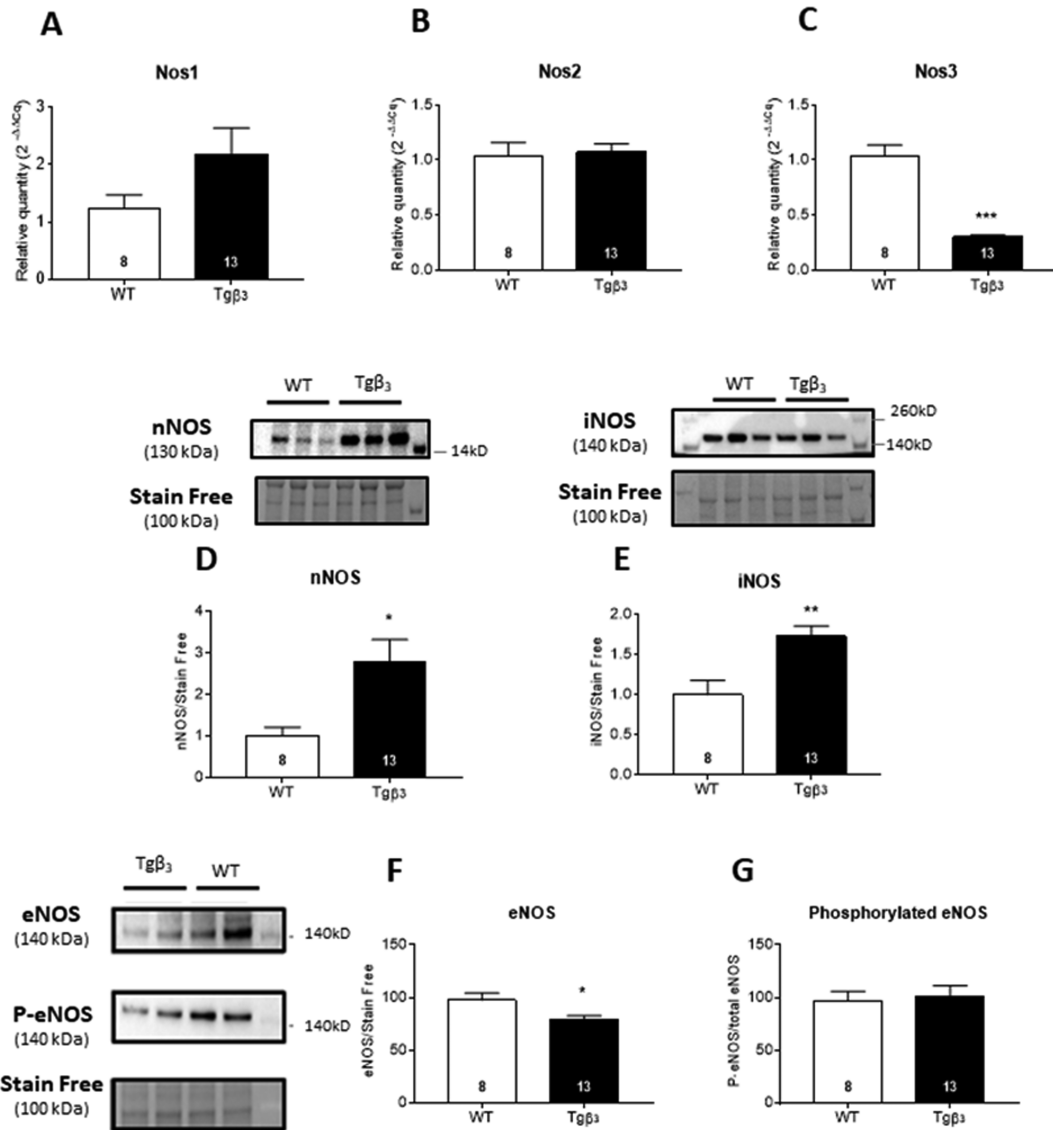
was performed at 15, 30, and 45 weeks of age. This investigation was performed on animals of both sexes, as well as on WT animals. We also investigated ovariectomized (OVX) female rats. We observed that WT and Tgβ_3 female rats—either OVX or non-OVX—display no alteration in their cardiac function during ageing (Supporting Information, *Tables S3* and *S4* and *Figure S2*). In contrast, Tgβ_3 male rats do show a diastolic dysfunction that develops during ageing and that persists. Because of this sex difference in the manifestation of cardiac defects, we decided to focus our attention on male animals. Therefore, only data from male WT and Tgβ_3 rats will be presented in this manuscript.

With regard to other physiological parameters, WT and Tgβ_3 male rats at 45 weeks of age presented similar weight and tibia length (Supporting Information, *Tables S5* and *S6*). Blood pressure assessment revealed that Tgβ_3 male rats did not show any significant modification in systolic (136.3 ± 4.0 mmHg for WT vs. 133.4 ± 4.6 mmHg for Tgβ_3), diastolic (95.3 ± 2.0 mmHg for WT vs. 92.7 ± 3.1 mmHg for Tgβ_3), or mean arterial pressure (109.0 ± 2.6 mmHg for WT vs. 106.3 ± 3.5 mmHg for Tgβ_3) (Supporting Information, *Table S7*).

In vivo investigation of cardiac function

Systolic function, evaluated by the calculated EF, remained normal in both WT and Tgβ_3 rats regardless of age (*Figure 5A*). Repeated measurements over time of early-to-late filing ratios (E/A) revealed that diastolic dysfunction is exacerbated

Figure 4 Vascular reactivity analysis. Concentration–response curves to isoproterenol were obtained by measuring contractility of wild-type (WT) (○, n = 4–5) and Tgβ₃ (■, n = 4–5) aorta (A), in the presence (plain line) or absence (dotted line) of endothelium. •NO (B) and $O_2^{•-}$ (C) production were evaluated by electron paramagnetic resonance spectroscopy in aorta at 45 weeks of age in WT (n = 4) and Tgβ₃ (n = 4). Data are expressed as mean ± standard error of the mean. $^*P < 0.05$.
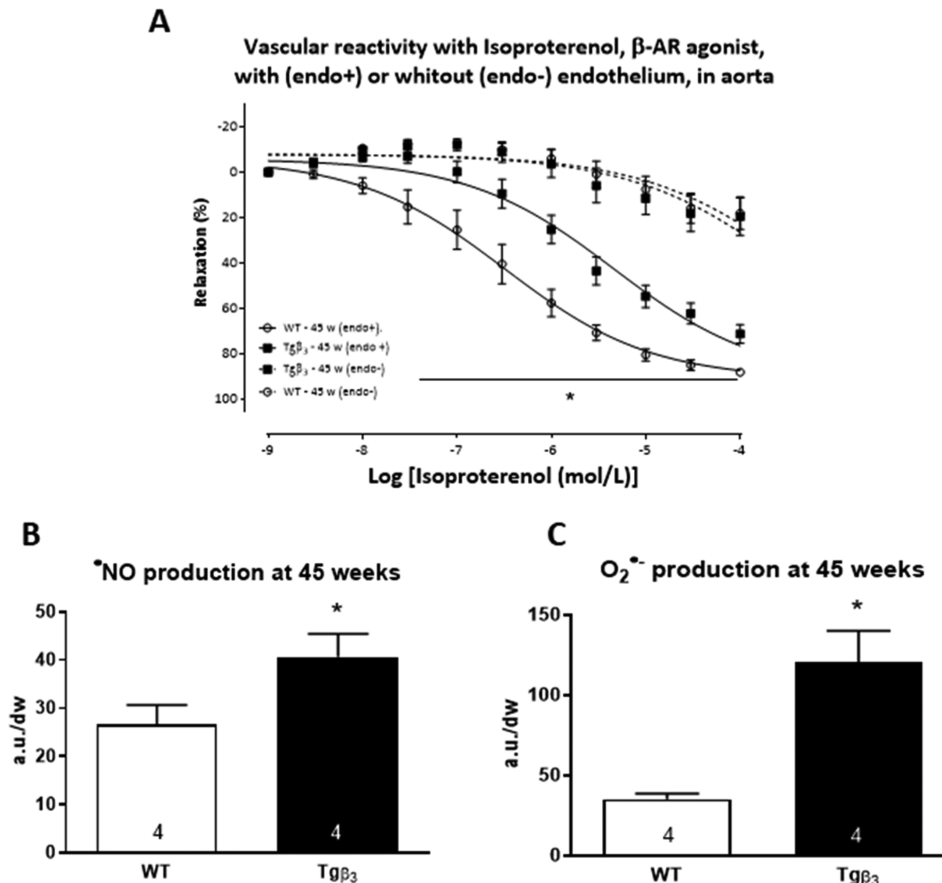
with a restrictive filling pattern over age. Indeed, at 30 and 45 weeks of age, the E/A ratio was significantly increased in Tgβ₃ rats (1.08 ± 0.04 for WT vs. 1.26 ± 0.05 for Tgβ₃; $P < 0.05$ for 30 weeks; and 1.15 ± 0.01 for WT vs. 1.33 ± 0.04 for Tgβ₃; $P < 0.05$ for 45 weeks) (*Figure 5B*). This increase in the E/A ratio was associated with the dilation of the left atrium (LA) (*Figure 5C*). Also, at 45 weeks of age, Tgβ₃ rats showed a significant increase in left ventricular end-diastolic pressure (LVEDP) (5.57 ± 1.23 mmHg for WT vs. 11.68 ± 1.11 mmHg for Tgβ₃; $P < 0.05$, *Figure 5D*). The E/A ratio is low: it is because the heart rhythm is high as a consequence of low anaesthesia, which favours fusion of E wave and A wave and artificially lowers the E/A ratio.

Ex vivo investigation of cardiac function

Intrinsic heart function was evaluated using an isolated working heart model. Under physiological conditions, Tgβ₃ hearts showed a significantly higher LVEDP (+50%), an increase in heart rate (+8%), and a decrease in systolic pressure (−9%) compared with WT animals. *In vivo* blood pressure values did not differ between the groups. The difference between

in vivo and *ex vivo* results is explain by the devoid of any neurohormonal modulation in isolated heart, and one cannot exclude that some circulating factors may, *in vivo*, modulate the cardiac function. Diastolic function of Tgβ₃ hearts was altered, as illustrated by the decrease in dP/dt_{min} (+10%), in relaxation time (+14%), and in diastolic filing period (−28%). The systolic function, systolic ejection period, and contraction time were not statistically different, while dP/dt_{max} was decreased (−10%) in Tgβ₃ hearts. Altogether, these modifications were not associated with cardiac output and coronary flow modification in Tgβ₃ hearts (Supporting Information, *Table S8*).

Ex vivo investigation of cardiac function under stress conditions

Response to β-adrenergic receptor stimulation

To study the β-adrenergic receptor stimulation occurring during stress-induced catecholamine release on cardiac function, the effect of increasing concentrations of isoproterenol was investigated on isolated WT and Tgβ₃ working hearts. The

Figure 5 Cardiac function. Evolution of systolic function (A) and diastolic function (B) between 15 and 45 weeks measured by echocardiography. Evaluation of the area of the left atrium at 45 weeks by echocardiography (C). Left ventricular pressure measurements at 45 weeks of wild-type (WT) (n = 7) and Tgβ$_3$ (n = 8) rats (D). Data are expressed as mean ± standard error of the mean. $^*P < 0.05$.
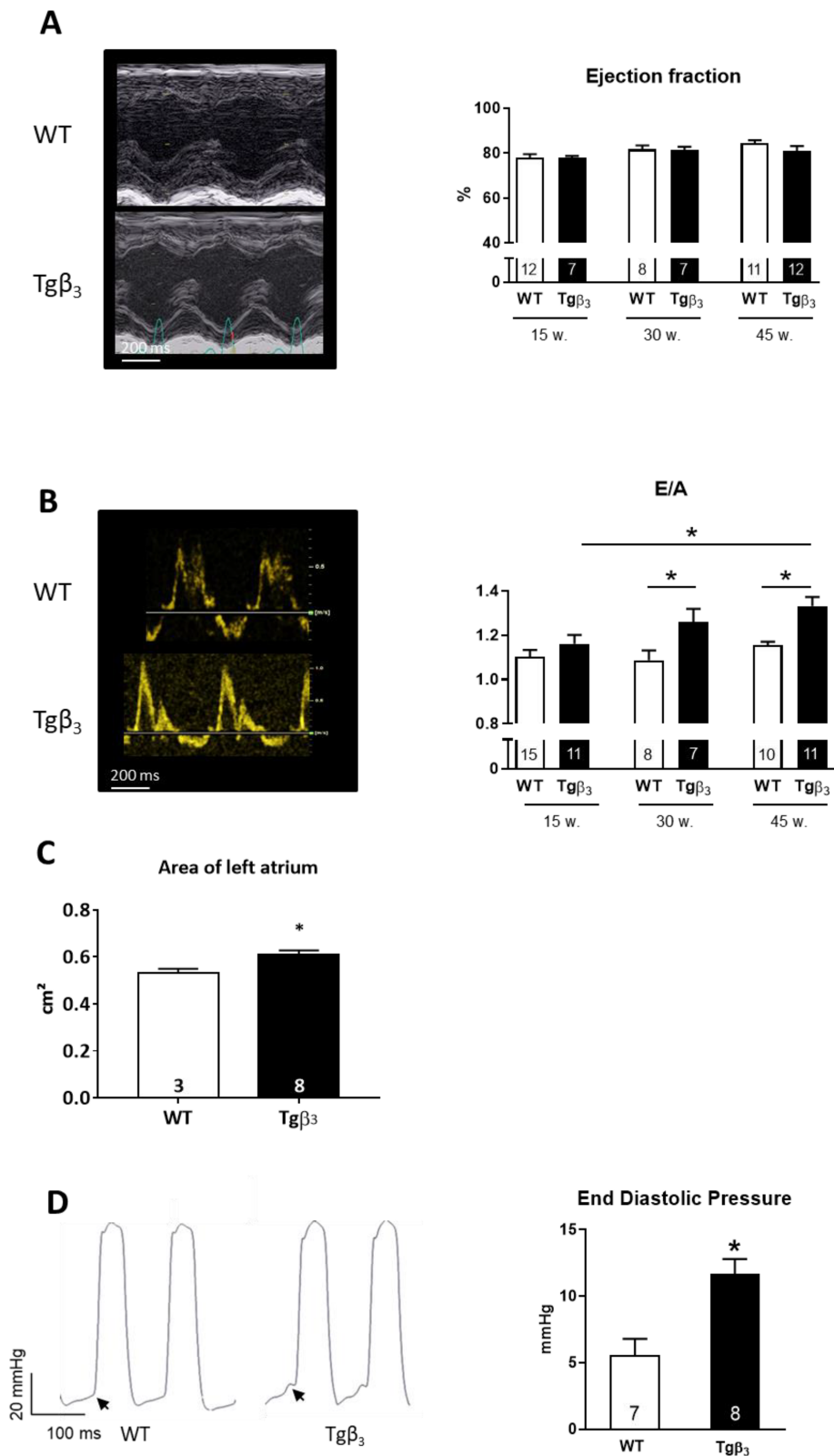
Figure 6 Isoproterenol concentration–response curve in isolated working heart. dP/dt_{max}, dP/dt_{min} (A), cardiac output (B), and aortic flow (C) were measured on wild-type (WT) (○, $n = 8$) and Tgβ₃ (■, $n = 8$). The effects of an afterload increase on cardiac function of WT (○, $n = 8$) and Tgβ₃ (■, $n = 8$) rats were evaluated on dP/dt_{max} and dP/dt_{min} rate (D), cardiac output (E), and aortic flow (F). The effects of a preload increase on cardiac function of WT (○, $n = 12$) and Tgβ₃ (■, $n = 13$) rats were evaluated through the study of dP/dt_{max} and dP/dt_{min} rate (G), cardiac output (H), and aortic flow (I). BL, baseline. Data are expressed as mean ± standard error of the mean. $^*P < 0.05$, $^{**}P < 0.01$, and $^{***}P < 0.001$ for WT vs. Tgβ₃.
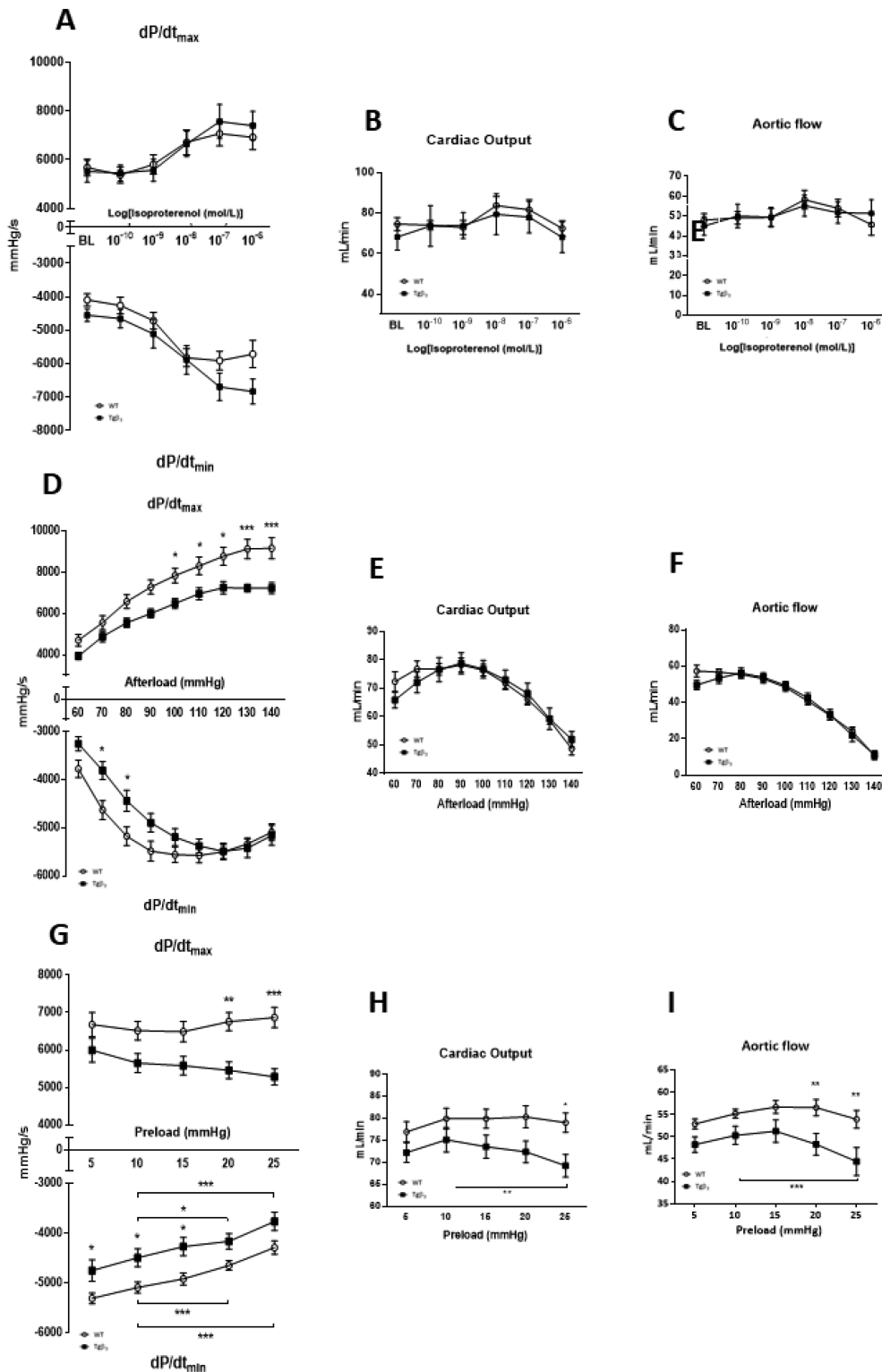
effects of isoproterenol were similar in both Tgβ$_3$ and WT hearts in terms of cardiac contraction and relaxation rate (*Figure 6A*), cardiac output (*Figure 6B*), and aortic flow (*Figure 6C*). These results are in agreement with the similar transcription levels of β$_1$-AR and β$_2$-AR expressed in both Tgβ$_3$ and WT rats (*Figure 1B*).

Response to pressure variation

An afterload increase was applied to reproduce *ex vivo* increases in peripheral resistance and to stimulate the systolic adaptation. From 100 mmHg, adaptation in contractility of Tgβ$_3$ hearts was impaired (for dP/dt_{max} at 14 mmHg: 9167 ± 510 mmHg/s for WT vs. 7234 ± 263 mmHg/s for Tgβ$_3$; $P < 0.05$) (*Figure 6D*). Cardiac outputs and aortic flows were similar in WT and Tgβ$_3$ hearts (*Figure 6E* and *6F*). In another study, a diastolic stress was applied by gradually increasing the preload in order to mimic pulmonary arterial pressure increase or on venous return. The preload increase induced a significant dP/dt_{min} elevation in both WT and Tgβ$_3$. However, WT hearts showed significantly elevated contractility, while the adaptive response of Tgβ$_3$ hearts was impaired (*Figure 6G*). In the presence of a high preload (25 mmHg), the ejection capacity of Tgβ$_3$ hearts was significantly decreased. We observed a 14% decrease in cardiac output (79.0 ± 2.2 mL/min for WT vs. 69.2 ± 2.6 mL/min for Tgβ$_3$; $P < 0.05$) (*Figure 6H*) and a decrease in aortic flow (*Figure 6I*). These results reveal that diastole duration and the heart capacity to work were blunted at the highest levels of preload in Tgβ$_3$ hearts.

Discussion

Endothelial overexpression of hβ$_3$-AR in our model is associated with an endothelial dysfunction along with a slow development of diastolic function alteration, an impaired filling pattern, and an increase in LVEDP. *In vivo* blood pressure and body weight do not differ between the two groups, suggesting that the diastolic dysfunction is observed without the presence of co-morbidities (hypertension, obesity, etc.) contrary to many models that induce HFpEF. The subtle cardiac impairment was exacerbated during stress conditions, especially when the diastolic function was challenged. Our data suggest that this animal model, with endothelial-localized alterations in signalling, develops diastolic dysfunction and endothelial alteration. Tgβ$_3$ rats display a progressive diastolic dysfunction, illustrated by the elevation of their E/A ratio with ageing, associated with an increased LVEDP. The slight but significant increase in collagen deposition (Supporting Information, *Figure S3*) observed in our model suggests that other parameters are implicated in left ventricular (LV) stiffness and diastolic dysfunction.[12] The absence of cardiac remodelling in male rats Tgβ$_3$ may be surprising. Indeed, the study of Shah et al.[13] have shown a high prevalence of hypertrophy of the left ventricle in HFpEF patient with diastolic dysfunction.

They also rely on the fact that hypertrophy of the LA is correlated with diastolic dysfunction. Ventricular hypertrophy is not associated with diastolic dysfunction in our model. But according to *Figure 5C*, hypertrophy of the LA is, however, well present in animals with diastolic dysfunction. In addition, other studies in animal models have shown that in the severe stages of diastolic dysfunction, an enlargement of the LA, potentially attributed to a LA–LV decoupling, has been observed.[14,15] Our study suggests that, in the early development of diastolic dysfunction, the onset of left atrial enlargement may be anterior to ventricular hypertrophy. Indeed, at 60 weeks, a sign of LV hypertrophy was observed with an increase of LV anterior wall depth (Supporting Information, *Figure S4A*).

It has been described that patients with diastolic dysfunction become pathological when the heart is submitted to a chronic or acute stress. In order to evaluate whether diastolic dysfunction is worsened under stress conditions, we used the working heart technique. This technique allowed us to study the impact of stress specifically on the systolic function, with an increase in afterload, or on the diastolic function, with an increase in preload and a pharmacological stress with isoproterenol. Tgβ$_3$ rat hearts displayed an alteration in contractility only when submitted to a high afterload level (130–140 mmHg). Alteration in contractility was not observed in echocardiographic study due to lower *in vivo* blood pressure (90–100 mmHg). These results suggest that if Tgβ$_3$ rat had hypertension, then they probably would develop a systolic dysfunction. After an increase in preload, Tgβ$_3$ hearts exhibit contractility and relaxation impairment, associated with a significant alteration of cardiac output. During exercise tolerance tests, HFpEF patients develop a strong LVEDP increase, and a decrease in stroke volume, indicating that diastolic function is severely worsened under stress conditions.[16] These results are in accordance with John et al. showing that diastolic function in patients is sensitive to preload variations[17] and indicate that heart function in these rats is altered specifically when diastolic function is evaluated.

The present study raises questions concerning the involvement of β$_3$-AR in diastolic dysfunction development. In the literature, β$_3$-AR has been reported to couple with NOS and to involve the Gαi–•NO–cGMP pathway,[10,18,19] which are known to be cardioprotective,[20] at least at a physiological expression level of β$_3$-AR. Earlier studies have indeed reported a beneficial effect of β$_3$-AR stimulation when expressed in cardiomyocytes (not endothelial cells): in acute disorders or anti-hypertrophic effect at an early stage of HF.[21] In acute disorders, it appears to produce a decrease in myocardial damage by decreasing mitochondrial permeability transition pore opening[22] or an anti-hypertrophic effect at an early stage of HF.[21] We report a deleterious effect of the long-term endothelial overexpression of β$_3$-AR suggesting a potential cell-specific effect of this pathway. Conversely, however, an elevated expression of β$_3$-AR, maybe associated to an increase in adrenergic stimulation, seems to be

detrimental. At the end-stage of HF, β_3-AR overexpression is associated with cardiac dysfunction,[23,24] suggesting that the cardiac effects of β_3-AR are much more complex than initially thought. In atrial fibrillation, recent studies show that chronic stimulation of β_3-AR may lead to iNOS uncoupling, leading to oxidative stress and atrial remodelling and atrial fibrillation.[25–27] In this report, the specific endothelial overexpression of the transgene allows us to suggest that the endothelium acts as a critical actor in the development of diastolic dysfunction. We have shown that the long-term overexpression of β_3-AR causes alterations in the $^\bullet$NO pathway and in calcium handling of endothelial cells. We have identified changes in NOS expression, in particular an increase in nNOS and iNOS levels occurring concomitantly with a decrease in eNOS expression level. The nNOS overexpression associated with β_3-AR stimulation in stress condition has been already described.[28] The decrease in eNOS expression can tentatively be explained by the increase of inflammation and $O_2^{\bullet-}$ expression that leads to eNOS uncoupling.[29] We also investigated the expression levels of cyto/chemokines in plasma and did not observe fluctuations of the concentrations of IL-6 and IL-1β. We observed a difference, but not significant, in the mean value of TNF-α, suggesting a potential low grade of inflammation at 45 weeks in Tgβ_3 rats (Supporting Information, *Figure S5*). The hypothetic low grade of inflammation could explain the increase of iNOS expression observed at 45 weeks and the eNOS uncoupling leading to endothelial dysfunction over the time.[30] But considering our results on inflammation, we cannot confirm the increase of inflammation and further study needs to be performed. This change in expression balance between the different NOS subtypes is associated with a significant increase in $^\bullet$NO production in endothelial cells. This overproduction was not due to the increase in the aortic internal diameters (Supporting Information, *Figure S6*). β_3-AR is believed to couple to eNOS and nNOS in endothelial cells, and an alteration in the relative expression levels of nNOS and eNOS in the β_3-AR overstimulation condition can explain the overproduction of $^\bullet$NO.[31] We postulate that, in the long run, the change in type of NOS coupling to β_3-AR and/or the overproduction of $^\bullet$NO, as a result of this change or of the overexpression of β_3-AR, is associated with a depletion in cellular energy store via different mechanisms such as the activation of poly-ADP ribose polymerase.[32] iNOS increase overexpression via β_3-AR could explain the endothelial dysfunction. Such a process may lead to a progressive alteration of the cardiac function. In addition, the overproduction of $^\bullet$NO has been associated with an increase in nitrosylation and reactive oxygen species production as supported by the increase in $O_2^{\bullet-}$ production in our model. Our results substantiate the involvement of the endothelium in the development of diastolic dysfunction as suggested earlier by Paulus and Tschöpe.[7] Recently, several studies confirmed the implication of endothelial cells, in both preclinical and clinical studies.[6] Indeed, Ebner et *al.*

demonstrated a diastolic dysfunction in a model of vascular eNOS dysfunction, suggesting that our animal model could be relevant to understand the pathophysiology underlying HFpEF.[33] Hence, we show that our rat model has important characteristics in common with HFpEF such as preserved EF, diastolic dysfunction, effort intolerance (*ex vivo* studies), age impact, and some structural anomalies as fibrosis, even though it lacks LV hypertension, and we did not observe alterations in renal or pulmonary vascular beds (Supporting Information, *Figure S7*). The transcriptomic study also confirmed interesting parallels between our model and HFpEF. We confirmed an alteration in the expression of the genes involved in collagen deposition, inflammation, metabolism, and calcium pathways (Supporting Information, *Figure S8*): a set of pathways also involved in the pathophysiology of diastolic dysfunction. The alteration in the $^\bullet$NO pathway, described in our model, might be linked potentially to other physiopathological mechanisms such as reactive oxygen production. The absence of cardiac dysfunction in female rats, including after ovariectomy, raises interesting questions regarding the implication of gender in our model. This issue was investigated in a recent study and concluded that in the HFpEF model with high-fat diet + N^ω-nitro-L-arginine methyl ester, the female sex is protective.[34] Now the issue will be to understand the mechanisms involved in this protection of the female sex in preclinical models. In HFpEF, treatment response seems to be different between women and men confirming the importance to study female and male animal in preclinical models. [35–37] The fact that only male rats develop the pathology is not fully understood in our study. Compared with other studies, we suppose that the addition of co-morbidities in female rats could increase the phenotype of diastolic dysfunction.

Even if Tgβ_3 rats have some similarities with HFpEF in humans: diastolic dysfunction, preserved EF, *in vivo* exercise intolerance (Supporting Information, *Figure S4B*), and a sign of cardiac hypertrophy (Supporting Information, *Figure S4A*), Tgβ_3 rats cannot be considered as a perfect HFpEF model because of the absence of pulmonary oedema (Supporting Information, *Figure S4C*) or more severe cardiac remodelling. However, the model remains valuable to understand the physiopathology of diastolic dysfunction and may become a greater model of HFpEF provided that other co-morbidities as hypertension or obesity are added to the phenotype.

In conclusion, the Tgβ_3 rat is an animal model of diastolic dysfunction. The pathology develops with ageing with a progressive filling impairment at rest, associated with diffuse fibrosis. Moreover, our data demonstrated a similar cardiac response of Tgβ_3 rats and HFpEF model when submitted to a stretch-induced stress, illustrating an altered adaptation to stress conditions. This new model confirms that an alteration of the physiology of endothelial cell signalling can lead to diastolic dysfunction. Our new rat model of diastolic dysfunction may help unravel part of the mechanisms involved

in diastolic dysfunction genesis. More importantly, it will help the pharmaceutical industry test some of their most promising leads for the prevention of the pathology.

Acknowledgements

Conflict of interest

None declared.

Funding

Supporting information

Additional supporting information may be found online in the Supporting Information section at the end of the article.

Figure S1. β_3-AR antibody (A). Western-Blot of β_3-AR protein at 15 and 45 weeks (B). β_3-AR protein level at 15 (Tgβ_3; n = 4) and 45 weeks (Tgβ_3; n = 5) (C). Data are expressed as mean ± SEM.
Figure S2. LV pressure measurements of 45 weeks WT (n = 8) and Tgβ_3 (n = 9) rats (A). Evolution of diastolic function between 15 and 45 weeks measured by echocardiography (B). Data are expressed as mean ± SEM.
Figure S3. Fibrosis quantification. (A) Cryosections were stained with picrosirius red and viewed under polarized light to distinguish type I (red) from type III (green) collagen. Representative views from WT and Tgβ_3 samples are presented. (B) Changes in Col3a1 transcript in WT (n = 7) and Tgβ_3

(n = 12) rats. (C) Changes in Col1a1 transcript in WT (n = 7) and Tgβ_3 (n = 13) rats. Data are expressed as mean ± SEM. *: $P < 0.05$.
Figure S4. (A) Left ventricular anterior wall depth in diastole at 60 weeks. (B) Treadmill tolerance test with the evaluation of travelled distance. (C) Lung weight (wet/dry). Data are expressed as mean ± SEM. *: $P < 0.05$.
Figure S5: (A) Rat IL-1β plasma concentration (B) Rat TNF-α plasma concentration (C) Rat IL-6 plasma concentration. Data are expressed as mean ± SEM. *: $P < 0.05$.
Figure S6. (A) Vascular density in myocardium (B) Mean area aorta. Representative views from WT and Tgβ_3 samples are presented. Data are expressed as mean ± SEM. *: P < 0.05.
Figure S7. Vascular injuries of lungs and kidneys from WT (n = 8) and Tgβ_3 (n = 9) rats. (A) Renal injuries were evaluated using the glomerular score (B). Data are expressed as mean ± SEM.
Figure S8. Protein expression of PLB (A), of serine 16 phosphorylated PLB (B), of SERCA2 (C), of RyR2 (D) and of serine 2,808 phosphorylated RyR2 (E) all evaluated on whole heart tissue extracts at 45 weeks in WT (n = 4–8) and Tgβ_3 (n = 10). Data are expressed as mean ± SEM. *: $P < 0.05$.
Table S1. Primers used for RT-qPCR experiments.
Table S2. Antibodies used for Western-Blot analyses.
Table S3. Cardiovascular parameters of WT and Tgβ_3 females at 45 weeks of age. Data are expressed as mean ± SEM.
Table S4. Arterial blood pressure values measured for WT and Tgβ_3 female rats at 45 weeks. Data are expressed as mean ± SEM.
Table S5. Physiological and cardiovascular parameters recorded for WT and Tgβ_3 males at 45 weeks of age. E/A: early-to-late filing ratio. Data are expressed as mean ± SEM *: $P < 0.05$.
Table S6. Cardiovascular parameters from WT and Tgβ_3 males at 15 and 30 weeks of age. Data are expressed as mean ± SEM.
Table S7. Arterial blood pressure values measured for WT and Tgβ_3 male rats at 45 weeks of age measured by arterial catheterism. Data are expressed as mean ± SEM.
Table S8. Characteristics of perfused isolated working hearts under physiological condition in WT and Tgβ_3 male rats at 45 weeks of age. Data are expressed as mean ± SEM. Afterload was set at 80 mmHg and preload at 12.5 mmHg *: $P < 0.05$.
45wk males differential

References

1. Dunlay SM, Roger VL, Redfield MM. Epidemiology of heart failure with preserved ejection fraction. *Nat Rev Cardiol* 2017; **14**: 591–602.

2. Ponikowski P, Voors AA, Anker SD, Bueno H, Cleland JGF, Coats AJS, Falk V, Gonzalez-Juanatey JR, Harjola VP, Jankowska EA, Jessup M. 2016 ESC guidelines for the diagnosis and treatment of acute and chronic heart failure. *Rev Espanola Cardiol Engl Ed* 2016; **69**: 1167.

3. Obokata M, Reddy YNV, Borlaug BA. Diastolic dysfunction and heart failure with preserved ejection fraction: understanding mechanisms by using noninvasive methods. *JACC Cardiovasc Imaging* 2020; **13**: 245–257.

4. Westermann D, Kasner M, Steendijk P, Spillmann F, Riad A, Weitmann K, Hoffmann W, Poller W, Pauschinger M, Schultheiss HP, Tschöpe C. Role of left ventricular stiffness in heart failure with normal ejection fraction. *Circulation* 2008; **117**: 2051–2060.

5. Jeong E-M, Dudley SC. Diastolic dysfunction. *Circ J Off J Jpn Circ Soc* 2015; **79**: 470–477.

6. ter Maaten JM, Damman K, Verhaar MC, Paulus WJ, Duncker DJ, Cheng C, van Heerebeek L, Hillege HL, Lam CSP, Navis G, Voors AA. Connecting heart failure with preserved ejection fraction and renal dysfunction: the role of endothelial dysfunction and inflammation. *Eur J Heart Fail* 2016; **18**: 588–598.

7. Paulus WJ, Tschöpe C. A novel paradigm for heart failure with preserved ejection fraction: comorbidities drive myocardial dysfunction and remodeling through coronary microvascular endothelial inflammation. *J Am Coll Cardiol* 2013; **62**: 263–271.

8. Schiattarella GG, Altamirano F, Tong D, French KM, Villalobos E, Kim SY, Luo X, Jiang N, May HI, Wang ZV, Hill TM, Mammen PPA, Huang J, Lee DI, Hahn VS, Sharma K, Kass DA, Lavandero S, Gillette TG, Hill JA. Nitrosative stress drives heart failure with preserved ejection fraction. *Nature* 2019; **568**: 351–356.

9. Gauthier C, Leblais V, Kobzik L, Trochu JN, Khandoudi N, Bril A, Balligand JL, le Marec H. The negative inotropic effect of beta3-adrenoceptor stimulation is mediated by activation of a nitric oxide synthase pathway in human ventricle. *J Clin Invest* 1998; **102**: 1377–1384.

10. Gauthier C, Tavernier G, Charpentier F, Langin D, le Marec H. Functional beta3-adrenoceptor in the human heart. *J Clin Invest* 1996; **98**: 556–562.

11. Chen Y, Park S, Li Y, Missov E, Hou M, Han X, Hall JL, Miller LW, Bache RJ. Alterations of gene expression in failing myocardium following left ventricular assist device support. *Physiol Genomics* 2003; **14**: 251–260.

12. Zile MR, Baicu CF, Ikonomidis JS, Stroud RE, Nietert PJ, Bradshaw AD, Slater R, Palmer BM, Van Buren P, Meyer M, Redfield M. Myocardial stiffness in patients with heart failure and a preserved ejection fraction: contributions of collagen and titin. *Circulation* 2015; **131**: 1247–1259.

13. Shah AM, Shah SJ, Anand IS, Sweitzer NK, O'Meara E, Heitner JF, Sopko G, Li G, Assmann SF, McKinlay S, Pitt B, Pfeffer MA, Solomon SD, TOPCAT Investigators. Cardiac structure and function in heart failure with preserved ejection fraction: baseline findings from the echocardiographic study of the Treatment of Preserved Cardiac Function Heart Failure with an Aldosterone Antagonist trial. *Circ Heart Fail* 2014; **7**: 104–115.

14. Wallner M, Eaton DM, Berretta RM, Borghetti G, Wu J, Baker ST, Feldsott EA, Sharp TE, Mohsin S, Oyama MA, von Lewinski D. A feline HFpEF model with pulmonary hypertension and compromised pulmonary function. *Sci Rep* 2017; **7**: 1–13.

15. Zakeri R, Moulay G, Chai Q, Ogut O, Hussain S, Takahama H, Lu T, Wang XL, Linke WA, Lee HC, Redfield MM. Left atrial remodeling and atrioventricular coupling in a canine model of early heart failure with preserved ejection fraction. *Circ Heart Fail* 2016; **9**: e003238.

16. Borlaug BA, Vojtech M, Russell Stuart D, Kristy K, Karel P, Becker Lewis C, Kass DA. Impaired chronotropic and vasodilator reserves limit exercise capacity in patients with heart failure and a preserved ejection fraction. *Circulation* 2006; **114**: 2138–2147.

17. John JM, Haykowsky M, Brubaker P, Stewart K, Kitzman DW. Decreased left ventricular distensibility in response to postural change in older patients with heart failure and preserved ejection fraction. *Am J Physiol Heart Circ Physiol* 2010; **299**: H883–H889.

18. Trappanese DM, Liu Y, McCormick RC, Cannavo A, Nanayakkara G, Baskharoun MM, Jarrett H, Woitek FJ, Tillson DM, Dillon AR, Recchia FA. Chronic β_1-adrenergic blockade enhances myocardial β_3-adrenergic coupling with nitric oxide-cGMP signaling in a canine model of chronic volume overload: new insight into mechanisms of cardiac benefit with selective β_1-blocker therapy. *Basic Res Cardiol* 2015; **110**: 456.

19. Birenbaum A, Tesse A, Loyer X, Michelet P, Andriantsitohaina R, Heymes C, Riou B, Amour J. Involvement of β_3-adrenoceptor in altered β-adrenergic response in senescent heart: role of nitric oxide synthase 1-derived nitric oxide. *Anesthesiol J Am Soc Anesthesiol* 2008; **109**: 1045–1053.

20. Jones SP, Bolli R. The ubiquitous role of nitric oxide in cardioprotection. *J Mol Cell Cardiol* 2006; **40**: 16–23.

21. Belge C, Hammond J, Dubois-Deruy E, Manoury B, Hamelet J, Beauloye C, Markl A, Pouleur AC, Bertrand L, Esfahani H, Jnaoui K. Enhanced expression of β_3-adrenoceptors in cardiac myocytes attenuates neurohormone-induced hypertrophic remodeling through nitric oxide synthase. *Circulation* 2014; **129**: 451–462.

22. García-Prieto J, García-Ruiz JM, Sanz-Rosa D, Pun A, García-Alvarez A, Davidson SM, Fernández-Friera L, Nuno-Ayala M, Fernández-Jiménez R, Bernal JA, Izquierdo-Garcia JL, Jimenez-Borreguero J, Pizarro G, Ruiz-Cabello J, Macaya C, Fuster V, Yellon DM, Ibanez B. β_3 adrenergic receptor selective stimulation during ischemia/reperfusion improves cardiac function in translational models through inhibition of mPTP opening in cardiomyocytes. *Basic Res Cardiol* 2014; **109**: 422.

23. Moniotte S, Kobzik L, Feron O, Trochu JN, Gauthier C, Balligand JL. Upregulation of β_3-adrenoceptors and altered contractile response to inotropic amines in human failing myocardium. *Circulation* 2001; **103**: 1649–1655.

24. Morimoto A, Hasegawa H, Cheng H-J, Little WC, Cheng C-P. Endogenous β_3-adrenoreceptor activation contributes to left ventricular and cardiomyocyte dysfunction in heart failure. *Am J Physiol-Heart Circ Physiol* 2004; **286**: H2425–H2433.

25. Dong J, Zhao J, Zhang M, Liu G, Wang X, Liu Y, Yang N, Liu Y, Zhao G, Sun J, Tian J, Cheng C, Wei L, Li Y, Li W. β_3-Adrenoceptor impairs mitochondrial biogenesis and energy metabolism during rapid atrial pacing-induced atrial fibrillation. *J Cardiovasc Pharmacol Ther* 2016; **21**: 114–126.

26. Sheng L, Shen Q, Huang K, Liu G, Zhao J, Xu W, Liu Y, Li W, Li Y. Upregulation of β_3-adrenergic receptors contributes to atrial structural remodeling in rapid pacing induced atrial fibrillation canines. *Cell Physiol Biochem* 2012; **30**: 372–381.

27. Wang X, Wang R, Liu G, Dong J, Zhao G, Tian J, Sun J, Jia X, Wei L, Wang Y, Li W. The β_3 adrenergic receptor agonist BRL37344 exacerbates atrial structural remodeling through iNOS uncoupling in canine models of atrial fibrillation. *Cell Physiol Biochem* 2016; **38**: 514–530.

28. Zhang Z, Ding L, Jin Z, Gao G, Li H, Zhang L, Zhang L, Lu X, Hu L, Lu B, Yu X. Nebivolol protects against myocardial infarction injury via stimulation of beta 3-adrenergic receptors and nitric oxide signaling. *PLoS ONE* 2014; **9**: e98179.

29. Karbach S, Wenzel P, Waisman A, Munzel T, Daiber A. eNOS uncoupling in cardiovascular diseases—the role of oxidative stress and inflammation. *Curr Pharm Des* 2014; **20**: 3579–3594.

30. Schiattarella GG, Rodolico D, Hill JA. Metabolic inflammation in heart failure with preserved ejection fraction. *Cardiovasc Res* 2020; **22**: 139.

31. Moens AL, Yang R, Watts VL, Barouch LA. Beta 3-adrenoreceptor regulation of nitric oxide in the cardiovascular system. *J Mol Cell Cardiol* 2010; **48**: 1088–1095.

32. Liu VWT, Huang PL. Cardiovascular roles of nitric oxide: a review of insights from nitric oxide synthase gene disrupted mice. *Cardiovasc Res* 2008; **77**: 19–29.

33. Ebner AKN, Brandt AZB, Weinert SPD, Ebner BAA, Wunderlich CWunderlich CE-AA, Strasser RH. Endothelial nitric oxide synthase-induced hypertrophy and Vascular dysfunction contribute to the left ventricular dysfunction in

caveolin-1$^{-/-}$ mice. *Can J Cardiol* 2017; **33**: 1716–1724.

34. Tong D, Schiattarella GG, Jiang N, May HI, Lavandero S, Gillette TG, Hill JA. Female sex is protective in a preclinical model of heart failure with preserved ejection fraction. *Circulation* 2019; **140**: 1769–1771.

35. Solomon SD, Rizkala AR, Lefkowitz MP, Shi VC, Gong J, Anavekar N, Anker SD, Arango JL, Arenas JL, Atar D, Ben-Gal T, Boytsov SA, Chen CH, Chopra VK, Cleland J, Comin-Colet J, Duengen HD, Echeverría Correa LE, Filippatos G, Flammer AJ, Galinier M, Godoy A, Goncalvesova E, Janssens S, Katova T, Køber L, Lelonek M, Linssen G, Lund LH, O'Meara E, Merkely B, Milicic D, Oh BH, Perrone SV, Ranjith N, Saito Y, Saraiva JF, Shah S, Seferovic PM, Senni M, Sibulo AS Jr, Sim D, Sweitzer NK, Taurio J, Vinereanu D, Vrtovec B, Widimský J Jr, Yilmaz MB, Zhou J, Zweiker R, Anand IS, Ge J, Lam CSP, Maggioni AP, Martinez F, Packer M, Pfeffer MA, Pieske B, Redfield MM, Rouleau JL, van Veldhuisen D, Zannad F, Zile MR, McMurray J. Baseline characteristics of patients with heart failure and preserved ejection fraction in the PARAGON-HF trial. *Circ Heart Fail* 2018; **11**: e004962.

36. Solomon SD, Rizkala AR, Gong J, Wang W, Anand IS, Ge J, Lam CSP, Maggioni AP, Martinez F, Packer M, Pfeffer MA, Pieske B, Redfield MM, Rouleau JL, van Veldhuisen DJ, Zannad F, Zile MR, Desai AS, Shi VC, Lefkowitz MP, McMurray JJV. Angiotensin receptor neprilysin inhibition in heart failure with preserved ejection fraction: rationale and design of the PARAGON-HF trial. *JACC Heart Fail* 2017; **5**: 471–482.

37. Borlaug BA, Anstrom KJ, Lewis GD, Shah SJ, Levine JA, Koepp GA, Givertz MM, Felker GM, LeWinter MM, Mann DL, Margulies KB. Effect of inorganic nitrite vs placebo on exercise capacity among patients with heart failure with preserved ejection fraction: the INDIE-HFpEF randomized clinical trial. *JAMA* 2018; **320**: 1764–1773.